REPORT R-810 FEBRUARY, 1978 UILU-ENG 78-2203

CSL COORDINATED SCIENCE LABORATORY

THERMODYNAMICS OF SURFACE CLUSTERS - DIRECT OBSERVATION OF Re_2 ON W(211)

KAJ STOLT
JOHN WRIGLEY
GERT EHRLICH

UNIVERSITY OF ILLINOIS - URBANA, ILLINOIS

UNCLASSIFIED

SECURITY CLASSIFICATION OF THIS PAGE *(When Data Entered)*

REPORT DOCUMENTATION PAGE		READ INSTRUCTIONS BEFORE COMPLETING FORM
1. REPORT NUMBER	2. GOVT ACCESSION NO.	3. RECIPIENT'S CATALOG NUMBER
4. TITLE *(and Subtitle)* THERMODYNAMICS OF SURFACE CLUSTERS – DIRECT OBSERVATION OF Re_2 ON W(211)		5. TYPE OF REPORT & PERIOD COVERED Technical Report 6. PERFORMING ORG. REPORT NUMBER R-810; UILU-ENG 78-2203
7. AUTHOR(s) Kaj Stolt, John D. Wrigley, and Gert Ehrlich		8. CONTRACT OR GRANT NUMBER(s) DMR 72-02937 DAAB-07-72-C-0259
9. PERFORMING ORGANIZATION NAME AND ADDRESS Coordinated Science Laboratory University of Illinois at Urbana-Champaign Urbana, Illinois 61801		10. PROGRAM ELEMENT, PROJECT, TASK AREA & WORK UNIT NUMBERS
11. CONTROLLING OFFICE NAME AND ADDRESS Joint Services Electronics Program		12. REPORT DATE February, 1978 13. NUMBER OF PAGES 46
14. MONITORING AGENCY NAME & ADDRESS*(if different from Controlling Office)*		15. SECURITY CLASS. *(of this report)* UNCLASSIFIED 15a. DECLASSIFICATION/DOWNGRADING SCHEDULE

16. DISTRIBUTION STATEMENT *(of this Report)*

Approved for public release. Distribution unlimited.

17. DISTRIBUTION STATEMENT *(of the abstract entered in Block 20, if different from Report)*

18. SUPPLEMENTARY NOTES

19. KEY WORDS *(Continue on reverse side if necessary and identify by block number)*

Surfaces
Atoms
Diffusion

20. ABSTRACT *(Continue on reverse side if necessary and identify by block number)*

Direct observations in the field ion microscope make it possible to determine the ratio of bound to dissociated dimers at equilibrium on a crystal surface. In principle, the thermodynamics of dissociation are accessible from the temperature dependence of this ratio. To establish the feasibility of such measurements, the kinetics governing changes in the dimer probabilities are worked out. This is done for isothermal processes, and for conditions typical of the quench from the temperature at which the equilibrium distribution is established to the temperature at which observations are made in the field ion

DD FORM 1 JAN 73 1473 EDITION OF 1 NOV 65 IS OBSOLETE

UNCLASSIFIED

SECURITY CLASSIFICATION OF THIS PAGE *(When Data Entered)*

20. ABSTRACT (continued)

microscope. Techniques are developed to correct for distortions of the equilibrium distribution during the quench. These rely upon measurements of the ratio of dimers in configuration 1 and 0 at low temperatures, combined with observations of P_D, the fraction dissociated at high temperatures. Experiments conforming to this scheme have been carried out for rhenium dimers on W(211). They yield internal energies of -3.7 ± 1.1 kcal/mole for rhenium dimers in configuration 1, and -2.3 ± 1.2 kcal/mole for dimers in configuration 0, measured relative to the energy of dissociated pairs. Our results suggest important contributions from indirect interactions.

UILU-ENG 78-2203

THERMODYNAMICS OF SURFACE CLUSTERS - DIRECT OBSERVATION OF Re_2 ON W(211)

by

Kaj Stolt, John D. Wrigley, and Gert Ehrlich

Supported by the National Science Foundation under Grant DMR 72-02937.

Supported by the Joint Services Electronics Program (U.S. Army, U.S. Navy, and U.S. Air Force) under Contract DAAB-07-72-C-0259.

THERMODYNAMICS OF SURFACE CLUSTERS - DIRECT OBSERVATION OF Re_2 ON W(211)[a]

by

Kaj Stolt[b], John D. Wrigley, and Gert Ehrlich

Coordinated Science Laboratory[c], Department of Metallurgy, and Department of Physics

University of Illinois at Urbana-Champaign

ABSTRACT

Direct observations in the field ion microscope make it possible to determine the ratio of bound to dissociated dimers at equilibrium on a crystal surface. In principle, the thermodynamics of dissociation are accessible from the temperature dependence of this ratio. To establish the feasibility of such measurements, the kinetics governing changes in the dimer probabilities are worked out. This is done for isothermal processes, and for conditions typical of the quench from the temperature at which the equilibrium distribution is established to the temperature at which observations are made in the field ion microscope. Techniques are developed to correct for distortions of the equilibrium distribution during the quench. These rely upon measurements of the ratio of dimers in configuration 1 and 0 at low temperatures, combined with observations of P_D, the

(a) Supported by the National Science Foundation under Grant DMR72-02937.

(b) IBM Postdoctoral Fellow. Present address: Department of Physical Metallurgy, Helsinki University of Technology.

(c) Supported by the Joint Services Electronics Program (U.S. Army, U.S. Navy, and U.S. Air Force) under Contract DAAB-07-72-C-0259.

fraction dissociated at high temperatures. Experiments conforming to this scheme have been carried out for rhenium dimers on W(211). They yield internal energies of -3.7 ± 1.1 kcal/mole for rhenium dimers in configuration 1, and -2.3 ± 1.2 kcal/mole for dimers in configuration 0, measured relative to the energy of dissociated pairs. Our results suggest important contributions from indirect interactions.

During the past decade, direct observations in the field ion microscope have yielded considerable quantitative information about the behavior of individual metal atoms diffusing on crystal surfaces.[1] More recently, these observations have been extended to clusters of interacting adatoms,[2] and for dimers we now have available a fairly detailed description of surface transport on the atomic level.[3-5] The emphasis of quantitative investigations has so far been upon the kinetics of atomic events. In contrast, the energetics governing the association of metal adatoms into clusters have not been extensively explored. A theory of the forces between adatoms on metal surfaces is beginning to emerge,[6-8] and some observations of cluster dissociation have been reported.[9] However, we do not yet have a quantitative picture of surface interactions between metal atoms, although these are fundamental to an understanding of cohesion in crystal layers.

In this paper, we address ourselves to the first quantitative determination of the thermodynamics governing dissociation of dimers on a crystal surface. The primary emphasis is upon the conditions and procedures appropriate for such thermodynamic studies. We concentrate upon one illustrative example - rhenium on the (211) plane of tungsten - to provide an indication of atomic forces in surface clusters. Much is already known about the chosen system from previous studies.[4] As appears from Fig. 1, the (211) plane is a channeled surface on which atomic motion is confined to one dimension. This simplifies both the experimental observations and their analysis. When two atoms are placed in adjacent

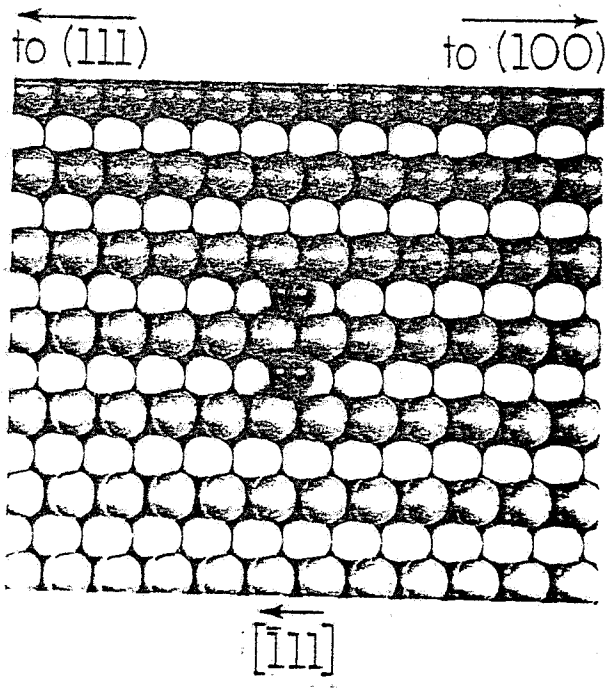

Fig. 1. Hard-sphere model of dimer on (211) plane of tungsten. Dimer movement is confined to [$\bar{1}$11] channels of close-packed atoms. Atomic spacing ℓ along channels - 2.74 Å; distance between neighboring channels - 4.48 Å.

channels of this plane and equilibrated, the probability of finding them dissociated rather than bound to each other provides a measure of the free energy change on dissociation; studies at different temperatures should then yield both the energy and entropy of dissociation.

Experimental determinations of this probability ratio are quite straightforward in the field ion microscope.[10] The sample surface is kept at the desired temperature for a time interval sufficient to establish thermal equilibrium, and then quenched to cryogenic temperatures. The distribution of adatoms over the surface is observed at low temperatures only, to avoid any possible perturbation of the system by the act of observation. It is assumed that the observations provide a close approximation to the equilibrium distribution at the chosen temperature. This assumption is critical. If the cooling rate is not high enough, extensive rearrangement of the adatoms may occur during the quench, invalidating the measurement. In fact, attaining high quenching rates in the field ion microscope presents quite a serious experimental problem. Even though our main concern is with equilibrium properties, we must therefore also analyze the kinetics governing the redistribution of dissociating dimers.

After a brief presentation of the thermodynamic formalism for dissociation and of some experimental particulars, we examine rate processes for dissociating dimers in Sec. III. The kinetics governing changes in the probability distribution of dimers on a surface are worked out under isothermal conditions, and are then adapted to treat changes during quenching. Based on this analysis, procedures are outlined (in III.C) to

allow for the distortion of the high temperature distribution on cooling. These procedures make possible meaningful studies of the thermodynamics of dimers on a surface. Actual thermodynamic measurements on rhenium dimers, which constitute the central theme of this effort, are presented in Sec. IV and V.

I. DISSOCIATION EQUILIBRIUM OF DIMERS

At the temperatures considered here, adatoms on the (211) plane of tungsten are confined to channels formed by surface atoms close-packed in the $[\bar{1}11]$ direction. When two adatoms are placed in adjacent rows of such a surface and equilibrated, the probability of finding the atoms at a distance $\underline{i}$ from each other is[11]

$$P_i = C(2-\delta_{i0})(L-i)\exp - W_i/kT. \qquad (1)$$

Here $\underline{i}$ denotes the separation between adatoms, measured in the direction of the channels, in units of the spacing ℓ along the $[\bar{1}11]$; L is the number of sites accessible to an atom in a channel, δ_{i0} is the Kronecker delta, and C is a normalization constant, to insure that

$$\sum_{i=0}^{L-1} P_i = 1 \qquad (2)$$

Interactions between the atoms enter through W_i, the potential of mean force; in our situation, it can be equated to the change in the Helmholtz free energy F on moving two adatoms, initially at an infinite separation, to a distance $\underline{i}$ from each other. Since the normalization constant C itself depends upon the temperature, measurements of P_i as a

function of the temperature T do not suffice to determine the interaction. Instead, it is necessary to take the ratio of two probabilities - one at distances so large that interactions between adatoms are negligible, the other at the separation $\underline{i}$ of interest. Based on our previous work, we will assume that once the distance between adatoms equals or exceeds two spacings along the $[\bar{1}11]$, interactions have dropped to zero and the two adatoms are free ($W_{i\geq 2} = 0$). Any pair for which $\underline{i} \leq 1$ is counted as bound.

The probability P_D that a pair be dissociated is now given by

$$P_D = \sum_{i=2}^{L-1} P_i = (L-1)(L-2)/2, \tag{3}$$

and the ratio P_1/P_D is just

$$\begin{aligned} P_1/P_D &= [2/(L-2)]\exp - W_1/kT \\ &= [2/(L-2)]\exp S_1/k \exp - E_1/kT \quad . \end{aligned} \tag{4}$$

Here and throughout this paper all thermodynamic quantities are referenced to the properties of dissociated pairs; the internal energy E_D and entropy S_D of dissociated dimers are therefore set equal to zero. A semi-logarithmic plot of P_1/P_D versus 1/T should yield both the internal energy and the entropy of pairs in state 1, provided the number of sites L in the diffusion channel is known. It must be noted, however, that apart from the statistical problems usual in quantitative studies of individual atoms, there is now the additional difficulty of establishing the temperature T to which the observed probabilities pertain. This will be discussed in Sec. III.

II. EXPERIMENTAL CONDITIONS - QUENCHING RATES

Our experiments hinge on the ability to distinguish dissociated from bound dimers. As indicated in Fig. 2, this is easily done in the field ion microscope. The procedures and equipment used to obtain field ion images, and especially to establish the separation between atoms in a cluster, have been detailed elsewhere.[4] Photographic recording of images has been improved, however, by using an Olympus OM2 camera, with f/1.2 optics, which automatically adjusts exposures to the correct time setting for Daylight Ektachrome film.

Most important for the present work is the extent to which the distribution of bound and dissociated pairs is altered by quenching to the cryogenic temperatures suitable for field ion microscopy. Such rearrangement depends upon how rapidly the sample cools after equilibration. This temperature decay has been measured for the two support loops used in this study. Both are made of .007 in. diameter tungsten; the end-to-end length is $\approx$ 8 cm for the first, and only $\approx$ 2 cm for the second.[12] During the quench, the resistance of the support is monitored by a 4-lead technique. The emf across the potential leads to the loop is displayed on an oscilloscope, as in Fig. 3. It is thus possible to follow rapid changes in the temperature of the support, which may exceed one hundred degrees per second. The time for the support to cool down to $\approx 300^{\circ}K$ is critical for freezing in place the high temperature distribution. During this interval, the cooling curve, shown in Fig. 3, can be approximated by the hyperbolic relation

$$1/T = 1/T_0 + bt \quad . \tag{5}$$

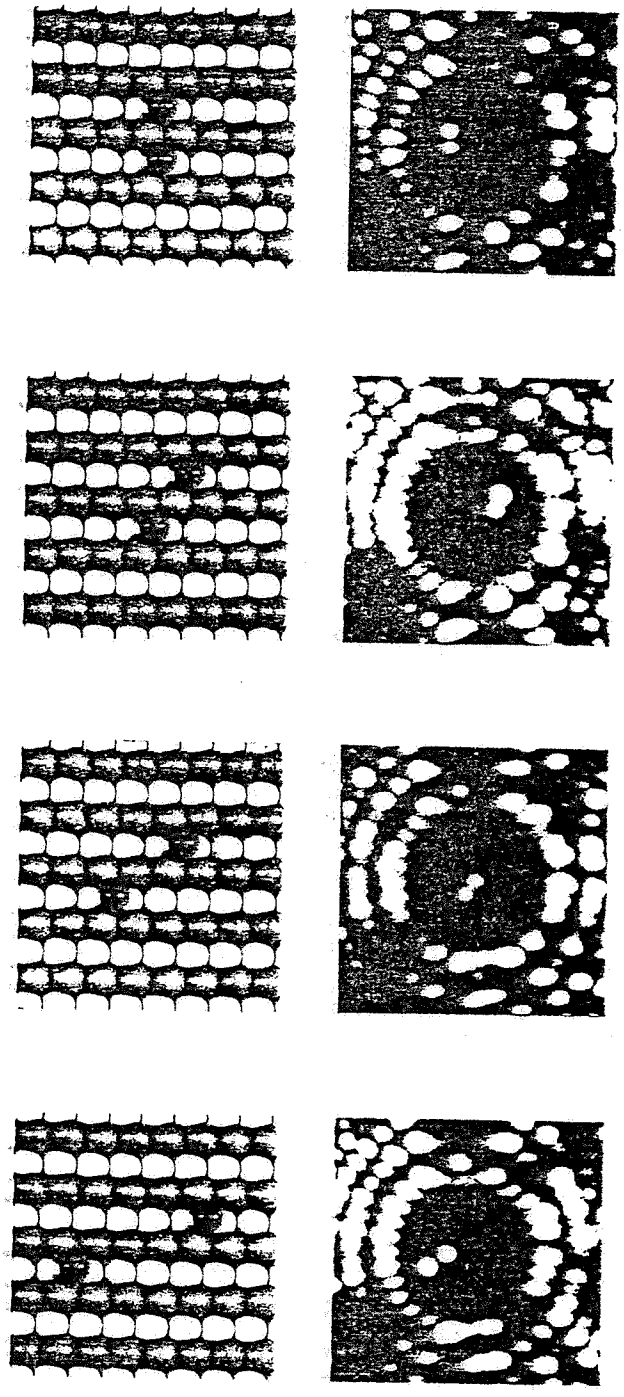

Fig. 2. Configurations of bound and dissociated rhenium dimers on W(211). Hard-sphere model on left, field ion image on right. Dimer configurations, from top to bottom: 0, 1, 2, and 4: the top two are bound, the bottom two free. Interatomic separation of atoms in dimer established by techniques in reference 4.

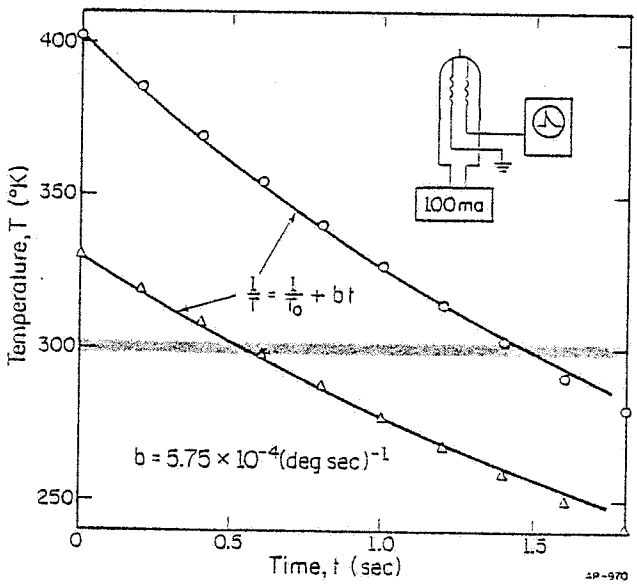

Fig. 3. Cooling curves for sample support after equilibration at T_0 = 330 and 402°K. Points indicate temperatures obtained from resistance measurements, solid curves are least-squares fit to $1/T = 1/T_0 + bt$. Shading shows temperatures at which dimer distrubutions are frozen in.

The decay rate parameter $\underline{b}$ is essentially independent of T_0, the initial temperature of the support loop. For the long support, $\underline{b} = 5.75 \times 10^{-4}$ $(\text{deg sec})^{-1}$; for the shorter loop, $\underline{b} = 3.0 \times 10^{-3}$ $(\text{deg sec})^{-1}$.

With the cooling rate established, it is now possible to assess the extent to which the original distribution, established in conformity with Eq. (4) by equilibration at a high temperature, is affected during the quench to the low temperatures at which observations are made.

III. KINETICS OF DIMER FORMATION AND DISSOCIATION

To understand how an equilibrium distribution of dimers is perturbed by changes in the temperature, the formalism for the kinetics of dimer dissociation at constant temperature is examined first. In III.B we then analyze the effects of quenching on an equilibrium distribution of model dimers. Finally, the implications of this kinetic analysis for studies of the dissociation equilibrium are examined, and techniques are devised for utilizing experimental observations in such a way as to circumvent changes in the actual high temperature distributions during cooling.

A. Isothermal Dissociation

1. Formalism

Migration of dimers in an infinite one-dimensional channel is readily described by noting the position of the center of mass, together with the configuration of the dimer[3,5]; the latter is given by the separation $\underline{i}$ between the two adatoms in the pair (measured in units of the atomic spacing ℓ along the channel). The conventions governing the rate constants for

atom jumps from one site to a specified neighboring site are indicated schematically in Fig. 4. The rate is denoted by α if the jump increases the pair separation, and by β if it causes a decrease. The subscript to the symbol indicates the configuration prior to the jump; jumps can occur only between adjacent sites.

The probability $p_{x,i}$ that the center of mass of a dimer in configuration $\underline{i}$ be at position x therefore changes in accord with[13]

$$\frac{dp_{x,i}}{dt} = \dot{p}_{x,i} = \alpha_{i-1}(p_{x-1,i-1} + p_{x+1,i-1}) - 2(\beta_i + \alpha_i)p_{x,i}$$

$$+ \beta_{i+1}(p_{x-1,i+1} + p_{x+1,i+1}) \qquad x = 0, \pm 1, \pm 2, \ldots , \quad (6)$$

where $\alpha_{-1} = \beta_0 = 0$. We are not really concerned with the position dependence of the probability, however; our emphasis is rather on the probability P_i of finding a dimer in a given state $\underline{i}$. By definition,

$$P_i \equiv \sum_x p_{x,i} \, . \quad (7)$$

Summing Eq. (6) over all values of x now gives the time dependence of the probability P_i:

$$\dot{P}_i = 2[\alpha_{i-1}P_{i-1} - (\alpha_i + \beta_i)P_i + \beta_{i+1}P_{i+1}]$$

$$i = 0,1,2,\ldots \, . \quad (8)$$

In a finite system the number of accessible configurations is limited. Henceforth, we confine ourselves to a set of K configurations, ranging from

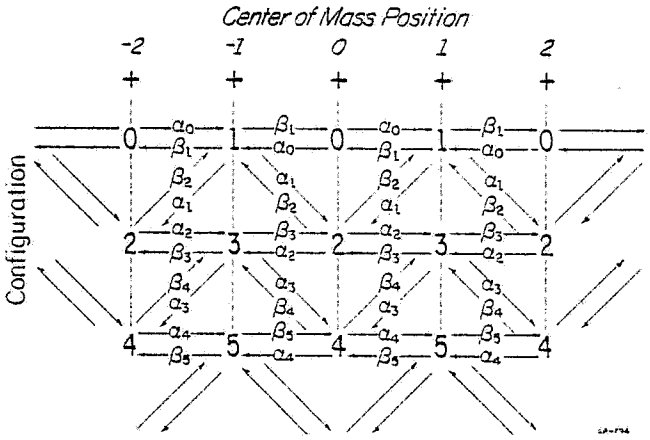

Fig. 4. Rate constants for jumps of dimers in one-dimensional diffusion. Center of mass positions are indicated by crosses and labelled with italic numbers. Arrows show atomic jumps allowed between nearest neighbor positions. Jump rates to higher configuration are given by α, to lower configuration by β; subscript labels the starting configuration.

$\underline{i} = 0$ to $\underline{i} = K-1$, and assume that there is no interchange with higher configurations, so that $\alpha_{K-1} = \beta_K = 0$. With this assumption, we are left with the equations

$$\begin{aligned}
\dot{P}_0 &= 2[-\alpha_0 P_0 + \beta_1 P_1] \\
\dot{P}_1 &= 2[\alpha_0 P_0 - (\alpha_1 + \beta_1)P_1 + \beta_2 P_2] \\
P_j &= 2[\alpha_{j-1} P_{j-1} - (\alpha_j + \beta_j)P_j + \beta_{j+1} P_{j+1}] \qquad j = 2,3,\ldots,K-2 \\
\dot{P}_{K-1} &= 2[\alpha_{K-2} P_{K-2} - \beta_{K-1} P_{K-1}] \quad .
\end{aligned} \tag{9}$$

The solution to this set of differential relations is well known;[14] it corresponds to the concentration of the i^{th} intermediate found in a sequence of K coupled, first-order chemical reactions, and is given by

$$P_i = \sum_{k=1}^{K} B_k A_{ik} \exp - \lambda_k t \quad . \tag{10}$$

The λ_k are eigenvalues of the matrix $2\underset{\sim}{M}$, where $\underset{\sim}{M}$ is defined as

$$\begin{bmatrix}
\alpha_0 & -\beta_1 & & & & & \\
-\alpha_0 & (\alpha_1 + \beta_1) & -\beta_2 & & & & \\
 & -\alpha_1 & (\alpha_2 + \beta_2) & -\beta_3 & & & \\
 & & & \vdots & & & \\
 & & & -\alpha_{K-3} & (\alpha_{K-2} + \beta_{K-2}) & -\beta_{K-1} \\
 & & & & -\alpha_{K-2} & \beta_{K-1}
\end{bmatrix} \tag{11}$$

The coefficients A_{ik} are given by the components of the corresponding eigenvector. Both the eigenvalues and eigenvectors can be evaluated by

standard methods.[15] The constants B_k are then determined from the initial conditions on the probabilities P_i.

It must be emphasized that the probabilities P_i found in Eqs. (10) describe dimers moving along infinite channels, but limited to configurations from 0 through K-1; that is, the maximum separation between atoms in a dimer is limited to K-1 atomic spacings. Experimental observations are actually made on channels having L accessible sites; these allow a maximum separation of L-1 spacings between partners in a pair. However, even if K were equated to L, Eqs. (10), as they stand, do not provide a satisfactory solution to our physical problem. This is evident on considering the steady state values for the probabilities P_i. In the steady state, that is for $\dot{P}_i = 0$, it is apparent from Eq. (9) that

$$P_{i+1}/P_i = \alpha_i/\beta_{i+1} \ . \tag{12}$$

If we limit ourselves to dimer separations $\underline{i}$ exceeding the range $\underline{f}$ of interatomic forces, then the rates α_i and β_{i+1} are equal, and it follows from Eq. (12) that

$$P_{i+1}/P_i = 1 \ , \qquad i \geq f.$$

However, for a channel of L sites we know from Eq. (1) that when $i \geq f$, and hence $W_i = 0$,

$$P_{i+1}/P_i = [L - (i+1)]/(L-i) \qquad i \geq f \ .$$

To satisfy this requirement, the probabilities given by Eq. (10) are weighted by ω_i, where

$$\omega_i = (L-i) / \sum_{i=0}^{L-1} (L-i)P_i \quad . \tag{13}$$

Reed[16] has demonstrated by Monte Carlo simulation that this procedure provides a satisfactory approximation to dimer dissociation on finite channels, even far removed from the steady state. The solutions given by Eqs. (10), weighted in accord with Eq. (13), will henceforth be used to describe the probabilities of model dimers at constant temperature.

2. Time Evolution of Probabilities for Model Dimers

In order to show how the probabilities P_i approach their steady state values, Eq. (10) has been evaluated for a model system, described in Fig. 5. This system is patterned loosely on the properties expected for Re_2 on the (211) plane of tungsten, as suggested by previous studies. In the model, interaction effects are neglected beyond configuration 1; that is, dimers with an interatomic separation of 2 spacings are assumed to behave as free atoms. The jump rate α of free atoms, and the rate β_1 at which dimers jump into the 0 configuration, are set equal to the values found in experiments[4] with rhenium on W(211). The temporal evolution of the probabilities, shown in Fig. 6, is specific for the model system. However, the particular choice of the rate constant β_1 does not significantly affect the outcome; a change in β_1 by a factor of two does not perceptibly change the plots, provided the ratio α_0/β_1 remains fixed.

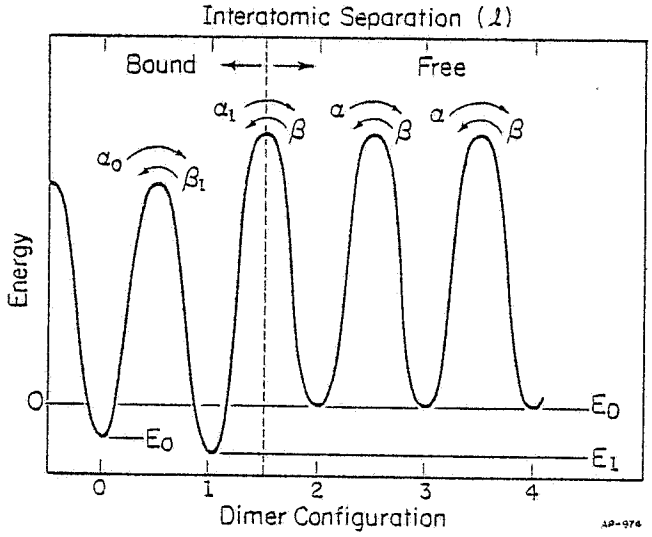

Fig. 5. Schematic potential diagram for model system. Dimers in configuration 2 and higher are completely dissociated; their potential energy E_D is taken as the zero of reference. Rate constants are assigned the following values: $\alpha_0/\beta_1 = 0.4 \exp 1234.6/R_GT$; $\alpha_1 = 3 \times \alpha \exp -3500/R_GT$, $\beta_1 = 2.5 \times 10^{12} \exp -18,300/R_GT \text{ sec}^{-1}$, $\alpha = 2.95 \times 10^{12} \exp -19,800/R_GT \text{ sec}^{-1}$; the last two rates are experimental quantities for rhenium on W(211). [4] $R_G = 1.987$ cal (deg mole)$^{-1}$.

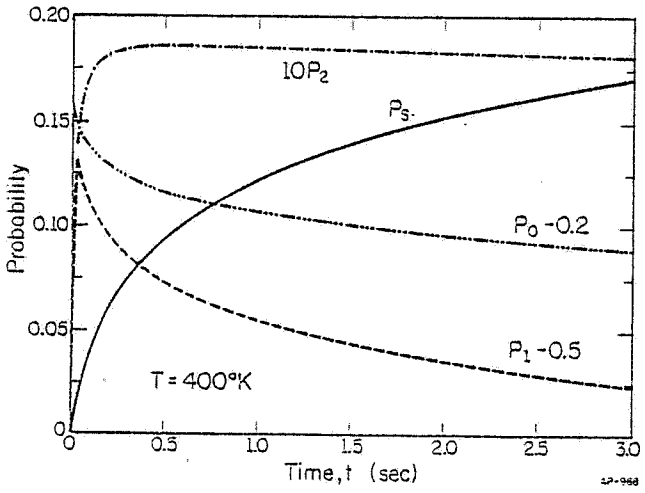

Fig. 6. Time evolution of dimer probabilities for model system at 400°K. To bring probabilities to a common scale, arbitrary constants are subtracted from P_0 and P_1; P_2 is multiplied by a factor of 10. $P_s \equiv 1 - (P_0 + P_1 + P_2)$.

The time dependence of the probabilities, which is displayed in Fig. 6 for a dimer starting in the 0 configuration, is complicated and has contributions from a number of exponential terms. However, equilibration between states 0 and 1 occurs instantly on the time scale appropriate to dissociation. Only .02 seconds after starting in the 0 configuration, the ratio P_1/P_0 is within 0.1% of the equilibrium value; a plot for dimers starting in the 1 configuration is indistinguishable from the one shown. The equilibration of the higher configurations takes considerably longer, and follows a course typified by the probability P_2 - a rapid initial rise, in which the equilibrium value is overshot, followed by a gradual diminution, as redistribution to the other configurations occurs. The sum total of the probabilities for states other than 0, 1 or 2 is included under the symbol P_s; this quantity (and also the probability P_D of finding a dimer dissociated) rises slowly but monotonically to its long term value.

B. Kinetics of Quenching

Of greater interest for this study are changes in the distribution which occur after equilibration, while the surface cools to the temperature at which observations are made. These changes are evaluated by approximating the actual hyperbolic cooling curve of the sample with a series of isothermals, Δ degrees apart, each terminated by an instantaneous drop to the next lower temperature. This procedure, suggested schematically in Fig. 7, makes it possible to determine the extent of distortion during the quench without extending the formalism of the previous section.

Estimates of such distortions are shown in Fig. 8 for our model system after equilibration at four temperatures at which significant dissociation occurs. From these curves it is evident that the procedure outlined in

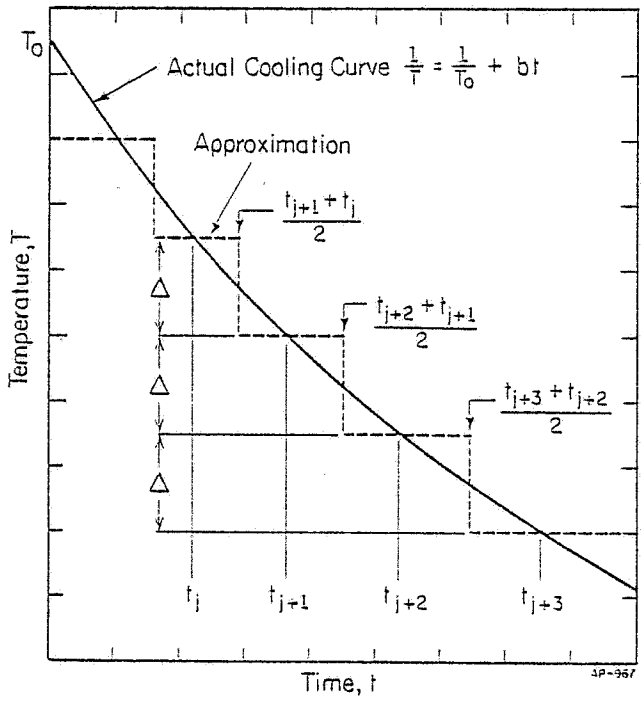

Fig. 7. Representation of cooling curve for sample support by isothermal intervals separated by step function drop of Δ degrees. For quantitative estimates of distortion during cooling, $\Delta \sim 2\text{-}4^{\circ}K$.

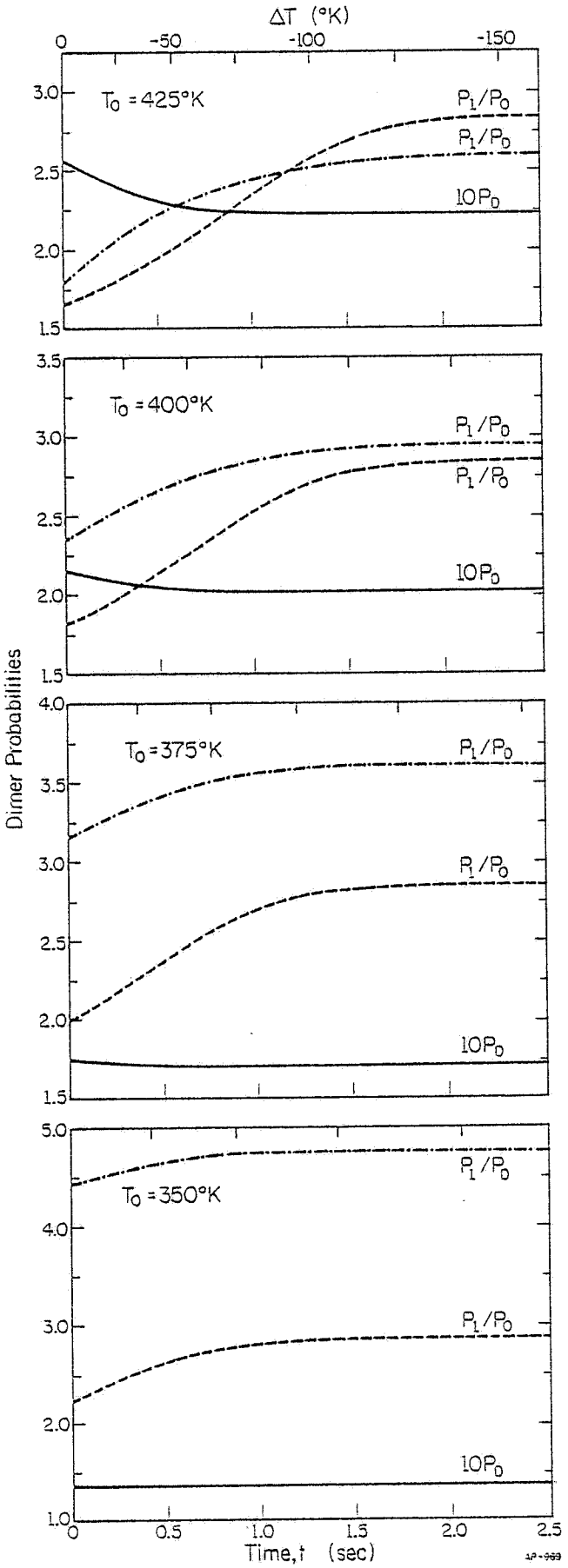

Fig. 8. Change in probabilities P_1/P_0, P_1/P_D, and P_D during quench of model dimers equilibrated at T_0. Temperature decay parameter $\underline{b} = 5.75 \times 10^{-4}$ (deg sec)$^{-1}$.

Sec. I for determining the thermodynamics of dissociation is not valid. Simply observing the ratio P_1/P_D after equilibration at different temperatures will not work: the distribution obtained by equilibration at high temperatures is significantly altered during the quench to the temperature of observation, even for equilibration at temperatures as low as $350^{\circ}K$. In large measure the problem arises from the rapid interconversion between states 0 and 1. As is apparent in Fig. 9, the conversion is significant even at temperatures below $350^{\circ}K$; only below $300^{\circ}K$ is the ratio P_1/P_0 frozen in.

The probability P_D of finding a dimer dissociated is much better behaved. Dissociation is the limiting step in establishing an equilibrium distribution, and stops quickly during a quench. The reverse process, recombination into a bound pair, faces two obstacles: the comparatively high barrier to diffusion for individual atoms in this system, and the need on the average to diffuse over an appreciable distance before encountering the other adatom in the adjacent channel. During a quench, these effects preserve the number of dimers that had dissociated at high temperatures. Even after equilibration at $425^{\circ}K$, the probability P_D is changed by only $\approx$ 12.5% during the subsequent cool-down. To the extent that we focus upon this quantity, valid thermodynamic information should therefore be attainable.

C. Analysis of Dissociation Data

Based on these calculations for model dimers, it is now possible to devise a scheme for properly analyzing real systems. In order to derive the thermodynamics of dissociation from Eq. (4), we require reliable data for P_1/P_D. Only P_D, however, can be derived from

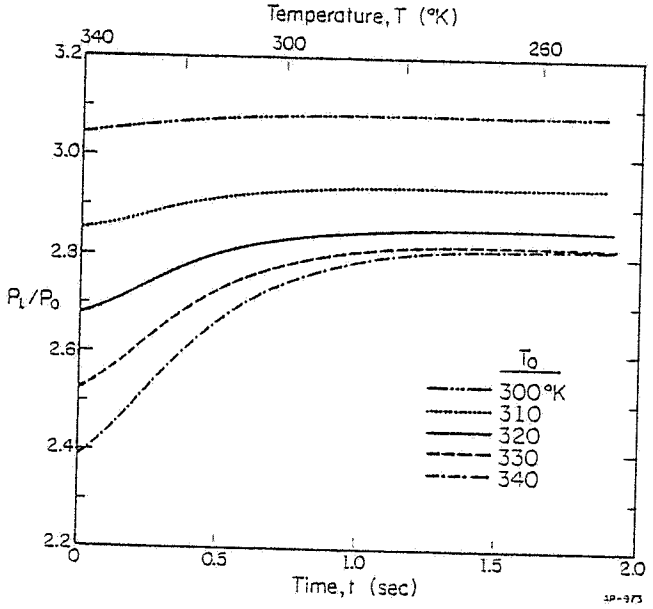

Fig. 9. Time evolution of P_1/P_0 for model dimers quenched after low temperature equilibration. Temperature scale appropriate only to $T_0 = 340^{\circ}K$. All values for $\underline{b} = 5.75 \times 10^{-4}$ (deg sec)$^{-1}$.

measurements at high equilibration temperatures without major distortion during quenching. We therefore estimate values of P_1 for the temperatures at which dissociation is significant by extrapolating P_1/P_0 from lower temperatures, at which distortion of this ratio is not too severe. These estimates are straightforward, provided sound data are available for the thermodynamics of dimers in state 1 relative to state 0.

Consider an experiment on a channel of length L, for which a total of M observations is available at a given equilibration temperature. Dimers are in state 1 in M_1 of these M observations, they are in state 0 in M_0 observations and are dissociated in M_D. Only M and M_D give significant information about dimer behavior at the equilibration temperature: the population of states 0 and 1 changes too much during quenching. Nevertheless, we can get M_0 and M_1 indirectly, by noting that

$$M_0 = (M-M_D)/(1+R_L)$$
$$M_1 = (M-M_D)R_L/(1+R_L) \quad . \tag{14}$$

Here the ratio M_1/M_0 for a channel of L sites is denoted by R_L. As already indicated, this ratio is derived by extrapolation from low temperatures. Thus, from Eq. (14) we can estimate M_0 and M_1 for the high temperatures at which dissociation is favored; this can be accomplished without the distortions inevitable in an attempt to observe the distribution after quenching to cryogenic temperatures.

The program for determining the thermodynamics of dimer dissociation is now clear. It requires measurements of P_D, the probability of finding

dimers dissociated after equilibration at high temperatures (in the vicinity of $\approx 400^{\circ}K$). Also needed are accurate values of P_1/P_0 for lower equilibration temperatures ($300^{\circ}K$ and less), to allow extrapolation of this ratio to temperatures at which dissociation is favored.

IV. EQUILIBRIUM BETWEEN RHENIUM DIMERS IN STATES 0 AND 1

Measurements of the relative population of rhenium dimers present in states 1 and 0 have previously been reported for W(211).[4] These studies were carried out over a wide range of temperatures, extending up to 390°K. For the higher temperatures, however, considerable distortion of the distribution must have occurred while the sample cooled to the temperature of observation. In fact, above 330°K, the previous data on P_1/P_0 (in Fig. 14 of reference 4) appear insensitive to the equilibration temperature; this strongly suggests that annealing during the quench, rather than the equilibration, dictated the observed distribution. More reliable values of $R \equiv P_1/P_0$ are therefore needed to allow extrapolation of this ratio into the dissociation regime.

A. Observations

Additional measurements of rhenium dimers in states 0 and 1 have been made at temperatures from 270° to 327°K. The observations are summarized in Table I, and are plotted in Fig. 10. Only statistical errors are indicated, derived from the standard relation[3]

$$\text{var } R = R^2/[(M-1)P_0P_1] \quad ; \tag{15}$$

this assumes that dissociation is negligible at these low temperatures.

On a channel of L sites, R_L, the ratio of pairs in state 1 to state 0, is related to the thermodynamic properties of the two states by

$$R_L = (P_1/P_0)_L = 2[(L-1)/L]\exp(S_1-S_0)/k \exp - (E_1-E_0)/kT \ . \tag{16}$$

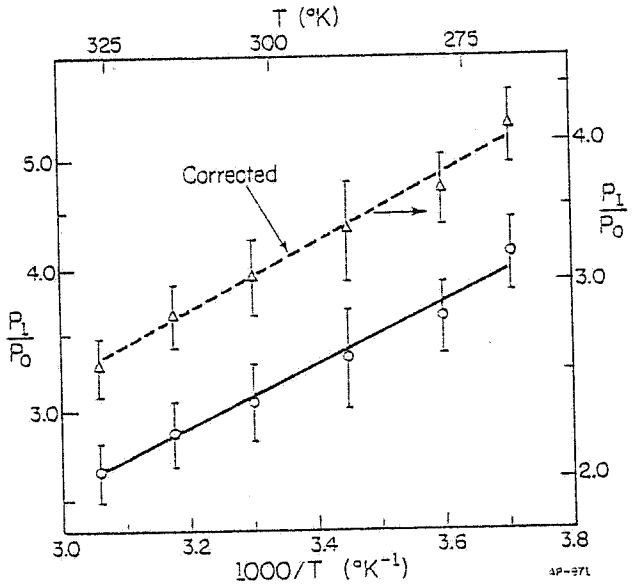

Fig. 10. Temperature dependence for ratio R of rhenium dimers in state 1, compared to state 0, on W(211). Raw data on bottom (ordinate at left) yields thermodynamic data in set (A). Values on top corrected for distortion during quench (ordinate at right), give data set (B). Error bars indicate standard deviation arising from statistical effects; curves obtained by least-squares fit to data points weighted by R^2/var R.

In the experiments, dimers are initially deposited in the center of the channels. At the low temperatures at which states 0 and 1 are equilibrated, dimers rarely move to the edge of the plane; when they do, the observations are disregarded. Adjustments for the length L of the channels are therefore not made in Eq. (16) - the ratio M_1/M_0 derived from the measurements is treated as equivalent to R_∞, the value of P_1/P_0 on an infinite channel. A semi-logarithmic plot of the observed values of P_1/P_0 against reciprocal temperature, in Fig. 10, yields

$$E_1-E_0 = -1.28 \pm .26 \text{ kcal/mole}$$
$$S_1-S_0 = -3.4 \pm .9 \text{ eu} \quad . \qquad \text{(A)}$$

B. Corrections

The extent to which the ratios P_1/P_0 taken at these low temperatures were distorted during the quench can be estimated, and corrected for, by taking advantage of the rate studies in Sec. III. We note that the ratio of the jump rates α_0 to β_1, which is required for such studies, is equal to R_∞. This ratio is calculated from Eq. (16) using the raw data in (A). The rate of diffusion of free dimers, α, as well as the jump rate β_1 from configuration 1 to 0, are set equal to the experimental values for rhenium on W(211).[4] Transitions from bound to dissociated pairs are assumed to occur at the rate $\alpha_1 = 3\alpha \exp - 3500/R_GT$, where R_G is the gas constant. Using these rate constants and the methods outlined in Sec. III, we can now estimate the changes in P_1/P_0 during the quench preceding field ion microscopy. The measured values of P_1/P_0 are corrected for these changes, and replotted to give a new estimate of the entropy and energy differences between states 0 and 1. Another cycle of corrections is then initiated,

using the new parameters to evaluate α_0/β_1, and this process is repeated until further correction does not significantly affect the energy difference estimated for rhenium dimers in state 0 and 1. As already noted, only the ratio of the rate constants α_0 to β_1, not their absolute value, affects the extent of distortion during a quench; this makes the iteration simple. For P_1/P_0, corrections even at 327°K amount to only 10% and one iteration brings the internal energy difference to within 1% of the final value.

Measurements of P_1/P_0, corrected in this way, are plotted in Fig. 10. The thermodynamic parameters for rhenium dimers derived from the corrected measurements are

$$E_1-E_0 = -1.40 \pm .26 \text{ kcal/mole}$$
$$S_1-S_0 = -3.8 \pm .9 \text{ eu} \quad . \qquad \text{(B)}$$

The difference in energy between state 1 and 0 found here is considerably larger than previously reported for the (211) plane of tungsten.[4] That is expected; earlier results were based on measurements extending to higher temperatures, at which redistribution during quenching dominated. If only data taken over lower temperatures are compared, then the earlier measurements agree with the present to well within one standard deviation.

V. EQUILIBRIUM BETWEEN BOUND AND DISSOCIATED RHENIUM DIMERS

With the thermodynamics of states 0 and 1 in hand, the ratio $R_L = (P_1/P_0)_L$ can be extrapolated to temperatures at which dimers are dissociated to an appreciable extent. Observations of the frequency with which dimers are dissociated, that is of M_D, combined with relation (14),

should now provide the information necessary for deriving the dissociation energy of dimers. One problem still remains - the ratio P_1/P_D as given by Eq. (4) depends upon the length L of the channel on which measurements were made. A scheme of reducing the various experiments to a standard length L_0 is presented in Sec. A. This makes it possible to analyze observations on the dissociation of rhenium dimers, which are presented in B.1. Finally, corrections for the distortions, which occur on quenching to the temperature at which field ion microscopy is done, are worked out in Sec. B.2, to yield the thermodynamic parameters for Re_2 on W(211).

A. Normalization of Data for Channel Length

Measurements of M_D are made on channels of different length, and it is first necessary to reduce them to a common channel length L_0. For final analysis of the data, we require the ratio M_1/M_D. It is not desirable to calculate this ratio for each experiment and then to combine the individual ratios, appropriately adjusted for differences in L and weighted, into one final average. Instead, it is preferable to first combine values of M_1 and M_D from different experiments into one grand total,[17] prior to taking the ratio M_1/M_D.

To accomplish this we take advantage of Eq. (4) to write

$$[(L-2)/2](M_1/M_D)_L = \exp - W_1/kT \ ;$$

here the subscript L explicitly indicates the length of the channel in a particular set of measurements. The left side is now independent of channel length, and it is clear that D_{L_0}, the ratio M_1/M_D referred to a channel of standard length L_0, can be deduced from experiments on channels of different lengths L according to

$$(M_1/M_D)_{L_0} = [(L-2)/(L_0-2)](M_1/M_D)_L = D_{L_0} \quad . \tag{17}$$

As already indicated in Sec. III, the ratio $(M_1/M_D)_L$ is not obtained from measurements of M_1 and M_D at the same temperature. M_D and M_1 are derived separately, M_D directly from dimer distributions at high temperatures, M_1 by extrapolation from data at lower temperatures. However, their ratio is readily corrected for the plane size.

Normalization is accomplished by an approximation. We write Eq. (14) in the form

$$(M_1)_{L_0} = M/(1+1/R_{L_0}+1/D_{L_0}) \quad . \tag{18}$$

The ratio R_{L_0} is available by extrapolation from low temperatures, in accord with Eq. (16); a value of D_{L_0} is derived from data on a channel of length L using Eqs. (14) and (17). For a channel of standard length L_0, the number of dimers which are dissociated or in state 1 can therefore be obtained from the measurements using the relations

$$(M_1)_{L_0} = M/\left[1 + \left(\frac{L_0}{L_0-1}\right)\frac{1}{R_\infty} + \left(\frac{L_0-2}{L-2}\right)\frac{1}{D_L}\right] \tag{19}$$

and

$$(M_D)_{L_0} = [(L_0-2)/(L-2)](M_1)_{L_0}/D_L \quad . \tag{20}$$

The values $(M_1)_{L_0,j}$ and $(M_D)_{L_0,j}$ so derived from the data in the j^{th} experiment are summed to finally give the desired ratio

$$(P_1/P_D)_{L_0} = \sum_j (M_1)_{L_0,j} / \sum_j (M_D)_{L_0,j} \quad . \tag{21}$$

Analysis of the statistical uncertainties in this estimate is complicated, but follows the procedures usual in the propagation of errors, with R_∞, the ratio P_1/P_0 on an infinite channel, and $(M_D)_L$ as independent variables.

B. Dissociation Equilibrium

1. Observations

The equilibrium between bound and dissociated rhenium dimers on the (211) plane of tungsten has been studied at temperatures ranging from 351° to 412°K. At temperatures lower than that, equilibration is inconveniently slow; at higher temperatures, the rate at which adatoms are lost from the plane is excessive. In the vicinity of 400°K, however, ≈ 20% of the dimers are dissociated, and the equilibrium between bound and dissociated pairs is easy to observe. After depositing a pair of rhenium adatoms in adjacent rows, they are equilibrated at the temperature of interest for a period ranging from 2 to 10 sec. This interval is chosen so that the adatoms in a dissociated dimer travel a distance comparable to the channel length and can therefore sense each other's presence. The state of the dimer is then examined after cooling to ≈ 20°K. This sequence is repeated, until one of the atoms is lost at the edge of the plane, or until a total of roughly 80 observations has been completed. Thereafter, the surface is field evaporated for general cleanliness, rhenium atoms are again evaporated onto the plane, and another measuring cycle is begun. Observations of dissociating dimers are shown in Fig. 11; the overall results are summarized in Table II.

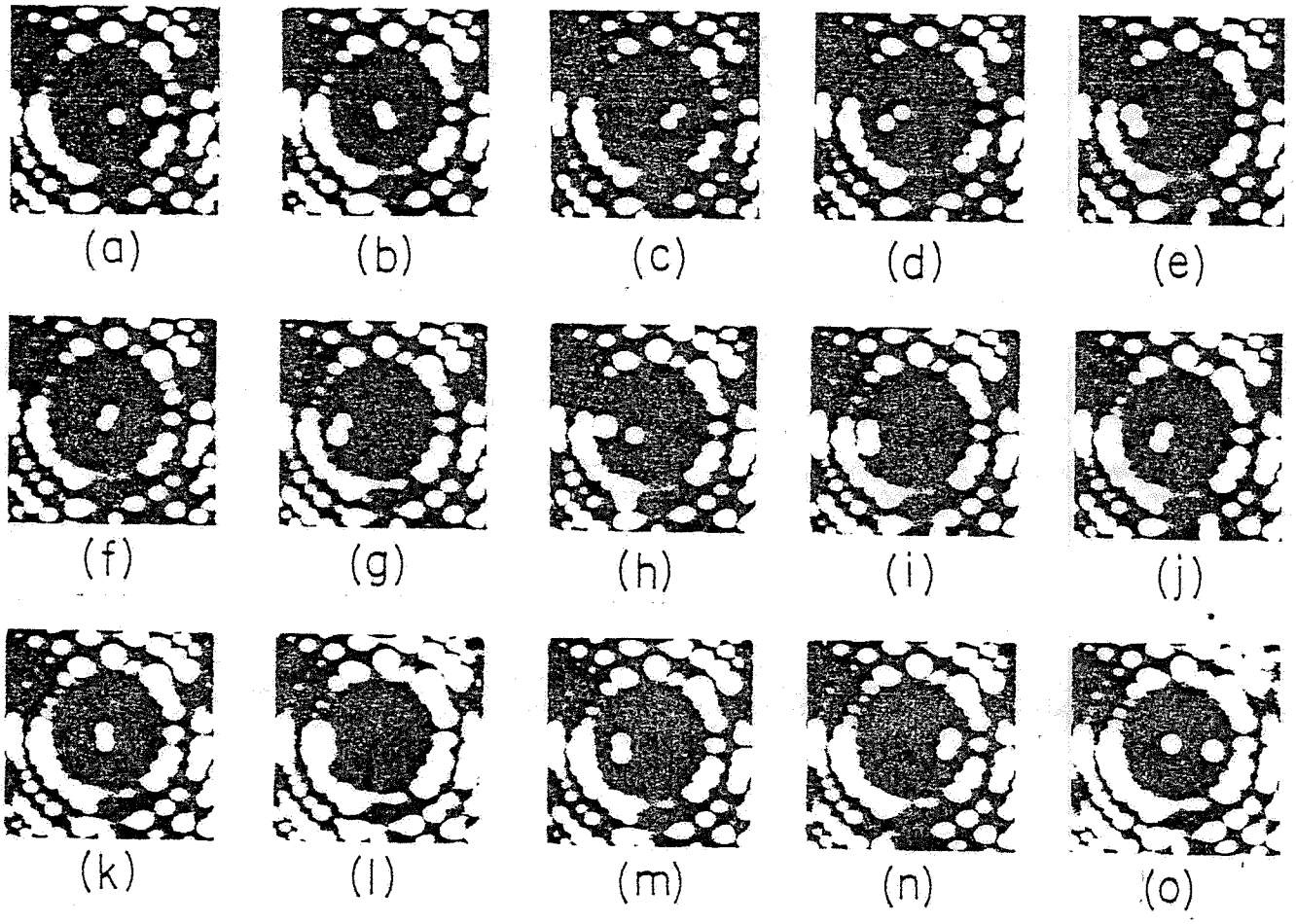

Fig. 11. Dissociation sequence for rhenium dimers on W(211). Observations after equilibration for 3 sec at 392°K are in chronological order. Labelling of atomic positions begins at left; channel length L = 27. (a) Position of adatom in top row - 29, position of adatom in bottom row - 19, configuration - 10, (b) 15, 16, 1 (c) 23, 21, 1 (d) 11, 8, 3 (e) 4, 5, 1 (f) 17, 16, 1 (g) 6, 5, 1 (h) 4, 11, 7 (i) 4, 4, 0 (j) 12, 11, 1 (k) 15, 15, 0 (l) 2, 2, 0 (m) 8, 8, 0 (n) 27, 26, 1 (o) 14, 25, 11. In quantitative analysis of the data, (l) not used as too close to edge.

Measurements were made on channels ranging in size from L = 17 to 32. The data are therefore normalized to a standard channel length, as outlined in the previous section; we adopt the value $L_0 = 25$, which is the mean for our experiments. A semi-logarithmic plot of $(P_1/P_D)_{L_0}$, derived from Eq. (21), versus 1/T now yields the thermodynamics of dissociation, in accord with Eq. (4). As stressed earlier, the ratio P_1/P_D not only involves measurements of dissociation, but also of the relative occurrence of states 1 and 0, obtained at lower temperatures. If we combine the raw data on dissociation, in Table II, with values of M_1/M_0 extrapolated from data set (B), then we obtain the raw dissociation plot shown in Fig. 12. This yields

$$E_1 = -3.3 \pm 1.1 \text{ kcal/mole}$$
$$S_1 = -1.6 \pm 2.9 \text{ eu} \quad . \qquad \text{(C)}$$

Only the statistical uncertainties arising from measurements of M_1/M_0 and of M_D, the number of dissociated dimers, have been included in the error bars. There is some uncertainty as well arising from possible errors in the lengths L of the channels. This uncertainty is small, however, amounting to only $\approx$ 1% of the standard error in the internal energy. The particular choice of L_0 to which the data are normalized also has little effect; a change of L_0 by 5 alters the estimate of the energy by only 1%.

2. Corrections

The raw values for the thermodynamics of rhenium dimers in state 1 are comparable to those of the model for which rate estimates were made in Section III.B. For that system, redistribution during the time

necessary for the sample to cool from 400°K to the temperature of observation lowered the number of dissociated pairs by ≈ 6%, quite a significant amount. Similar effects must be operating to distort the dissociation data for rhenium dimers. The number of dissociated pairs has there been corrected by the iterative method used on the ratio P_1/P_0 in Sec. IV. B. As the first step, the ratio α_0/β_1 is adjusted to the values of E_1-E_0 and S_1-S_0 in set (B). The energy E_1 of the model dimers is left at -3.5 kcal/mole, and the rate constants β_1 and α are fixed at the original values. Calculations of the changes in P_D on quenching from the actual equilibration temperatures are made, and the experimental data are corrected to yield an improved estimate of the thermodynamics of dissociation. The rate α_1, which corresponds to the transition from bound to free dimers, is adjusted to fit the new values of E_1 and S_1, and another cycle of correction is initiated. A total of three cycles is enough to converge on the corrected values plotted in Fig. 12, which give

$$E_1 = -3.7 \pm 1.1 \text{ kcal/mole}$$
$$S_1 = 2.8 \pm 2.9 \text{ eu} \quad . \qquad \text{(E)}$$

We consider these to be the preferred estimates for the thermodynamics of rhenium pairs in the 1 configuration on the W(211). Two things should be noted. The parameters of state 0 and 1 do not sensitively affect our estimates for the thermodynamics of dissociation; a 10% change in E_1-E_0 causes less than a 1% change in E_1. Also, the various corrections for distortion during quenching increase the internal energy by 15% at most; this is a small effect compared to the statistical uncertainty.

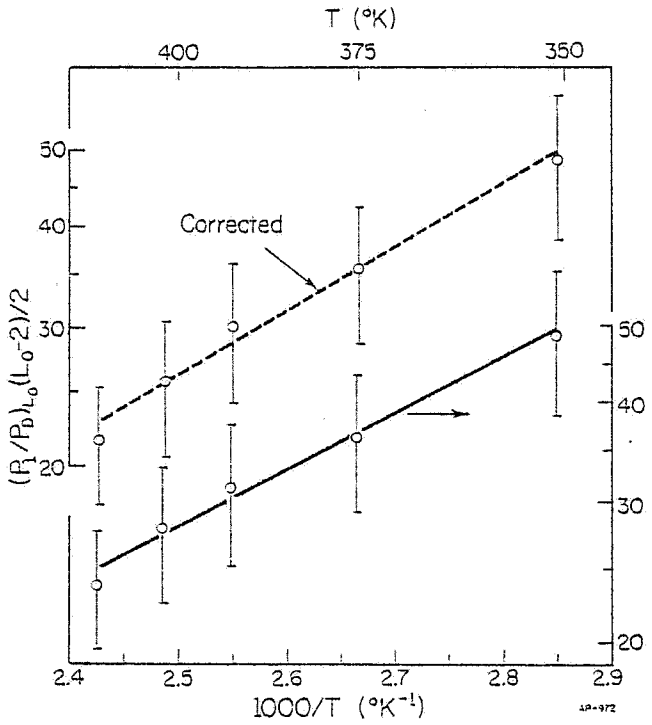

Fig. 12. Temperature dependence of dissociation equilibrium for rhenium dimers. Bottom curve for raw dissociation data (y-axis at right) yields thermodynamic parameters in set (C). Top curve (y-axis at left) shows dissociation data corrected for distortion during quench; this yields data in (D). Error bars indicate standard deviation σ due to statistical errors in observations; curves obtained by least-squares fit to points weighted by y^2/σ^2.

SUMMARY

The measurements reported here serve to define the energetics of rhenium dimers on the (211) plane of tungsten. Only one assumption enters the analysis of dissociation - that dimers in configuration 2 and higher can be treated as completely dissociated. The number of dimers observed in this configuration is small, however. An approximate analysis of dissociation is therefore possible, based on the alternative assumption that only dimers in configurations higher than 2 are dissociated. This changes the dissociation energy by less than 10%, an amount small on the scale of the statistical scatter. The specific assumptions about the range of atomic interactions thus do not significantly affect the results on dissociation

The observations of the relative occurrence of dimers in states 1 and 0 reveal an unexpected effect - the entropy of the former is considerably lower. To interpret this properly, it would be desirable to compare the entropy of configuration 0 and 1 with that of dissociated dimers. Unfortunately, the scatter in the dissociation results is still too large for this. The internal energies of dimers are in better shape. Compared with dissociated dimers, we have

$$E_1 = -3.7 \pm 1.1 \text{ kcal/mole}$$
$$E_0 = -2.3 \pm 1.2 \text{ kcal/mole} \quad .$$

The cohesive energy of rhenium pairs on the (211) thus is small, on the order of magnitude expected of van der Waals interactions. What is surprising is the difference between dimers in the 0 and 1 configuration.

The energy of the 0 state is significantly higher than of the 1; in the former, the interatomic separation is 4.48 Å compared to 5.25 Å in the 1 state. At close distances, repulsive interactions can be expected due to dipole-dipole interactions between adatoms polarized by the substrate. For adatoms with a net dipole of 1 D (a value characteristic of tungsten adatoms[18] on the (110) plane of tungsten), such repulsion increases the energy by only $\sim$ 160 cal/mole at 4.5 Å. This is not of the right magnitude to account for the observed energy difference between dimers in configuration 0 and 1. Moreover, it must be emphasized that other dimers[4], for which the energetics on W(211) have not yet been quantitatively examined, show a strong preference for the 0 state as compared to the 1. Such a pronounced chemical specificity is not expected for dipole-dipole repulsions. Indirect interactions must therefore be responsible for these distinctive energy differences. Additional information about these interactions should be available soon from kinetic measurements underway in this laboratory on rhenium clusters. We defer further discussion till then.

The primary purpose of the present study has been to demonstrate that thermodynamic data can be derived by direct observation of metal clusters at a surface. With this capability established, it would now be desirable to have quantitative information, similar to that presented here for rhenium on W(211), concerning the behavior of chemically different adatoms. This should make it possible to discern trends in atomic forces depending upon the electronic structure of the atoms interacting at a surface.

ACKNOWLEDGEMENTS

The experiments and accompanying analyses were possible only through the extensive help of R. B. Bales, R. T. Gladin, and W. I. Lawrence. We are also indebted to D. A. Reed, for measurements of the cooling curves and for many discussions, to S. Abrams for data analysis, and to Lynn Rathbun, for his incisive comments.

TABLE I. POPULATION OF RHENIUM DIMERS IN CONFIGURATIONS 0 AND 1

T	M_0	M_1	L	t(sec)
270[a]	45	212	25	20
	20	84	25	30
	44	126	25	30
	20	57	25	30
	38	171	25	30
	32	171	25	30
278[b]	9	36	24	120
	11	33	20	120
278[a]	16	61	25	60
	17	60	25	60
	17	61	25	60
	56	133	25	20
	31	152	25	20
	18	77	25	20
	42	173	25	20
290[b]	9	34	23	60
	4	28	19	90
	9	30	20	60
290[a]	16	61	25	60
	17	60	25	60
	16	48	25	30
	44	130	25	10
303[b]	9	31	22	40
	10	26	18	60
	5	26	20	60
	2	14	21	60
303	2	14	25[a]	30
	5	11	25[a]	30
	7	39	25[a]	30
	35	119	25[a]	20
	34	68	25[a]	20
	20	76	25[a]	20
	36	101	28	20
	30	75	25[a]	10
315[b]	10	29	25	30
	8	24	20	40
	10	19	21	40
	10	27	22	60
315	30	92	31	10
	38	84	30	15
	38	110	24	10
	36	96	26	10
	18	33	24	10
	25	110	24	10
	50	158	30	5
327[b]	10	22	22	30
	7	27	21	30
	17	32	23	30
327	38	116	32	10
	36	94	26	10
	38	70	25	10
	66	166	27	10
	40	136	31	10
	61	167	32	5

[a] Only a rough indication of channel length L available.

[b] Temperature decay parameter $\underline{b} = 5.75 \times 10^{-4}$ (deg sec)$^{-1}$; for all other measurements, $\underline{b} = 3.0 \times 10^{-3}$ (deg sec)$^{-1}$.

TABLE II. DISSOCIATION EQUILIBRIUM OF RHENIUM DIMERS ON W(211)

T	M_0	M_1	M_D	L	t	T	M_0	M_1	M_D	L	t
351	10	29	6	27	10	392[a]	11	23	15	31	5
	9	25	8	29	10	402	13	42	16	28	3
	20	41	9	28	10		13	15	6	17	2
	9	24	6	26	10		11	46	12	19	2
	13	45	4	27	10		12	20	9	20	2
	10	24	18	27	10		7	41	6	18	2
	25	49	6	29	10		8	15	7	21	2
	4	14	6	29	10		13	23	7	20	2
375	4	15	4	19	10		10	29	5	20	2
	3	6	4	20	10		11	27	9	23	2
	32	66	12	23	10		5	17	4	23	2
	3	14	2	21	10	412	12	34	13	25	2
	19	31	7	21	10		4	7	10	28	2
	24	62	20	22	10		1	21	5	27	2
	8	27	8	23	10		9	29	11	29	2
	19	31	7	23	10		5	22	5	28	2
	15	11	6	21	10		3	11	6	28	2
392	26	64	18	29	3		4	14	7	28	2
	3	13	6	26	3		8	26	6	28	2
	7	21	8	29	5		9	20	16	28	2
	10	24	16	28	3	412[a]	20	60	30	28	3
	8	22	8	27	3		27	59	31	32	3
	7	19	4	25	3						
	12	50	5	26	3						

[a]Temperature decay parameter $\underline{b} = 3.0 \times 10^{-3}$ $(\text{deg sec})^{-1}$. For all other measurements, $\underline{b} = 5.75 \times 10^{-4}$ $(\text{deg sec})^{-1}$.

REFERENCES

1 Much of this work has been reviewed by D. W. Bassett, Surf. Sci. 53, 74 (1975).

2 For a recent review, see G. Ehrlich, Surf. Sci. 63, 422 (1977).

3 D. A. Reed and G. Ehrlich, J. Chem. Phys. 64, 4616 (1976).

4 K. Stolt, W. R. Graham, and G. Ehrlich, J. Chem. Phys. 65, 3206 (1976).

5 J. D. Wrigley, D. A. Reed, and G. Ehrlich, J. Chem. Phys. 67, 781 (1977).

6 T. B. Grimley, Proc. Phys. Soc. Lond. 90, 751 (1967); ibid. 92, 776 (1967).

7 T. L. Einstein and J. R. Schrieffer, Phys. Rev. B 7, 3629 (1973); T. L. Einstein, Phys. Rev. B 16, 3411 (1977).

8 Reviews of the theory have been given by (a) J. R. Schrieffer, in Dynamic Aspects of Surface Physics, ed. by F. O. Goodman (Editrice Compositori, Bologna, 1974),p. 250; (b) T. B. Grimley, Prog. Surf. Membrane Sci. 9, 71 (1975).

9 D. W. Bassett and D. R. Tice, Surf. Sci. 40, 399 (1973); also in The Physical Basis of Heterogeneous Catalysis, ed. by E. Drauglis and R. I. Jaffee (Plenum, New York, 1975), p. 23.

10 The technical aspects of field ion microscopy are covered by E. W. Müller and T. T. Tsong, Field Ion Microscopy (American Elsevier, New York, 1969).

11 W. R. Graham and G. Ehrlich, Phys. Rev. Lett. 32, 1309 (1974).

[12] The length of the support is a compromise, influenced by two competing effects: for a long loop, the temperature distribution is more uniform at the sample, allowing more precise determinations of the equilibration temperature; however, cooling is more rapid for shorter loops.

[13] This follows from Eq. (A1) of reference 5, with rate constants conforming to the conventions in Fig. 4 of the present paper.

[14] See, for example, E. R. Lapwood, Ordinary Differential Equations (Pergamon, Oxford, 1968), Sec. 3.4.

[15] J. H. Wilkinson, The Algebraic Eigenvalue Problem (Clarendon Press, Oxford, 1965); J. H. Wilkinson and C. Reinsch, Linear Algebra (Springer, New York, 1971), p. 227.

[16] D. A. Reed, To be published.

[17] This avoids problems in properly weighting the results of a single experiment.

[18] K. Besocke and H. Wagner, Phys. Rev. B 8, 4597 (1973).

FIGURE CAPTIONS

Fig. 1. Hard-sphere model of dimer on (211) plane of tungsten. Dimer movement is confined to $[\bar{1}11]$ channels of close-packed atoms. Atomic spacing ℓ along channels-2.74 Å; distance between neighboring channels - 4.48 Å.

Fig. 2. Configurations of bound and dissociated rhenium dimers on W(211). Hard-sphere model on left, field ion image on right. Dimer configurations, from top to bottom: 0, 1, 2, and 4; the top two are bound, the bottom two free. Interatomic separation of atoms in dimer established by techniques in reference 4.

Fig. 3. Cooling curves for sample support after equilibration at T_0 = 330 and 402°K. Points indicate temperatures obtained from resistance measurements, solid curves are least-squares fit to $1/T = 1/T_0 + bt$. Shading shows temperatures at which dimer distributions are frozen in.

Fig. 4. Rate constants for jumps of dimers in one-dimensional diffusion. Center of mass positions are indicated by crosses and labelled with italic numbers. Arrows show atomic jumps allowed between nearest neighbor positions. Jump rates to higher configuration are given by α, to lower configuration by β; subscript labels the starting configuration.

Fig. 5. Schematic potential diagram for model system. Dimers in configuration 2 and higher are completely dissociated; their potential energy E_D is taken as the zero of reference. Rate constants are assigned the following values: $\alpha_0/\beta_1 = 0.4 \exp 1234.6/R_GT$; $\alpha_1 = 3 \times \alpha \exp -3500/R_GT$, $\beta_1 = 2.5 \times 10^{12} \exp -18{,}300/R_GT \text{ sec}^{-1}$, $\alpha = 2.95 \times 10^{12} \exp -19{,}800/R_GT \text{ sec}^{-1}$; the last two rates are experimental quantities for rhenium on W(211).[4]
$R_G = 1.987$ cal (deg mole)$^{-1}$.

Fig. 6. Time evolution of dimer probabilities for model system at $400^{\circ}K$. To bring probabilities to a common scale, arbitrary constants are subtracted from P_0 and P_1; P_2 is multiplied by a factor of 10. $P_s \equiv 1 - (P_0+P_1+P_2)$.

Fig. 7. Representation of cooling curve for sample support by isothermal intervals separated by step function drop of Δ degrees. For quantitative estimates of distortion during cooling, $\Delta \sim 2\text{-}4^{\circ}K$.

Fig. 8. Change in probabilities P_1/P_0, P_1/P_D, and P_D during quench of model dimers equilibrated at T_0. Temperature decay parameter $\underline{b} = 5.75 \times 10^{-4}$ (deg sec)$^{-1}$.

Fig. 9. Time evolution of P_1/P_0 for model dimers quenched after low temperature equilibration. Temperature scale appropriate only to $T_0 = 340^{\circ}K$. All values for $\underline{b} = 5.75 \times 10^{-4}$ (deg sec)$^{-1}$.

Fig. 10. Temperature dependence for ratio R of rhenium dimers in state 1, compared to state 0, on W(211). Raw data on bottom (ordinate at left) yields thermodynamic data in set (A). Values on top corrected for distortion during quench (ordinate at right), give data set (B). Error bars indicate standard deviation arising from statistical effects; curves obtained by least-squares fit to data points weighted by R^2/var R.

Fig. 11. Dissociation sequence for rhenium dimers on W(211). Observations after equilibration for 3 sec at $392^{\circ}K$ are in chronological order. Labelling of atomic positions begins at left; channel length L = 27. (a) Position of adatom in top row - 29, position of adatom in bottom row - 19, configuration - 10, (b) 15, 16, 1 (c) 23, 21, 1 (d) 11, 8, 3 (e) 4, 5, 1 (f) 17, 16, 1 (g) 6, 5, 1 (h) 4, 11, 7 (i) 4, 4, 0 (j) 12, 11, 1 (k) 15, 15, 0 (1) 2, 2, 0 (m) 8, 8, 0 (n) 27, 26, 1 (o) 14, 25, 11. In quantitative analysis of the data, (1) not used as too close to edge.

Fig. 12. Temperature dependence of dissociation equilibrium for rhenium dimers. Bottom curve for raw dissociation data (y-axis at right) yields thermodynamic parameters in set (C). Top curve (y-axis at left) shows dissociation data corrected for distortion during quench; this yields data in (D). Error bars indicate standard deviation σ due to statistical errors in observations; curves obtained by least-squares fit to points weighted by y^2/σ^2.